Accelerated Publications

Structure of the Metal−Water Complex in Ras·GDP Studied by High-Field EPR Spectroscopy and ^{31}P NMR Spectroscopy‡

Martin Rohrer,§ Thomas F. Prisner,§ Oliver Brügmann,§ Hanno Käss,|| Michael Spoerner,⊥ Alfred Wittinghofer,@ and Hans Robert Kalbitzer*,⊥

Institute for Physical and Theoretical Chemistry, University of Frankfurt, Frankfurt, Institute for Physical Chemistry, University of Darmstadt, Darmstadt, Institute for Biophysics and Physical Biochemistry, University of Regensburg, Regensburg, and Max-Planck-Institute for Molecular Physiology, Dortmund, Germany

Received September 14, 2000; Revised Manuscript Received December 4, 2000

ABSTRACT: The small GTPase Ras plays a key role as a molecular switch in the intercellular signal transduction. On $Mg^{2+} \rightarrow Mn^{2+}$ substituted samples, the first ligand sphere of the metal ion in the inactive, GDP-bound Ras has been studied by continuous wave EPR at 94 GHz (W-band). Via replacement of normal water with ^{17}O-enriched water, the ^{17}O−^{55}Mn superhyperfine coupling was used to determine the number of water ligands bound to the metal ion. In contrast to EPR data on frozen solutions and X-ray data from single crystals where four direct ligands to the metal ion are found, the wild-type protein has only three water ligands bound in solution at room temperature. The same number of water ligands is found for the mutant Ras(T35S). However, for the alanine mutant in position 35 Ras(T35A) as well as for the oncogenic mutant Ras(G12V), four water ligands can be observed in liquid solution. The EPR studies were supplemented by ^{31}P NMR studies on the Mg^{2+}·GDP complexes of the wild-type protein and the three mutants. Ras(T35A) exists in two conformational states (1 and 2) with an equilibrium constant $K_1(1,2)$ of approximately 0.49 and rate constants k_{1-1} which are much smaller than 40 s^{-1} at 298 K. For wild-type Ras and Ras(T35S), the two states can also be observed with equilibrium constants $K_1(1,2)$ of approximately 0.31 and 0.21, respectively. In Ras(G12V), only one conformational state could be detected.

The Ras[1] proteins are central molecular switches in cellular signal transduction, regulating important processes such as cell differentiation and proliferation. In up to 30% of all human tumors, specific mutations of Ras proteins can be found. In the resting cell, normal Ras exists mainly in the inactive form with GDP bound together with a Mg^{2+} ion in its active center. This GDP is exchanged for GTP by guanine nucleotide exchange factors (GEFs) in response to growth factor-related stimuli. The activated Ras protein in its GTP form transmits the signals by direct interaction with the Ras-binding domains of downstream targets such as the Raf-kinase. An excessive response to the signal is suppressed by the interaction of Ras with GTPase-activating proteins (GAPs) which deactivate the Ras protein by hydrolysis of the bound GTP to GDP (*1*, *2*). Since the bound nucleotides control the activation state of the protein, a detailed knowledge of their interactions with the surrounding is of general importance. The phosphate groups of GDP are directly interacting with the functional groups of the protein, as well as with the divalent ion Mg^{2+} bound in the active center and with several water molecules. In principle, from the published X-ray structures, a detailed view of these interactions can be obtained (*3*−*5*). However, as we could show by ^{31}P NMR spectroscopy for the effector loop in Ras·GppNHp, the conformation found in the crystal is not necessarily the dominant and/or unique conformation in solution (*6*).

Most contributions published so far are concerned with the "on" state of Ras with GTP bound. Nevertheless, for an understanding of the switching mechanism, the detailed knowledge about the "off" state with GDP bound is of similar

‡ Part of this work was presented at the XIX International Conference on Magnetic Resonance in Biological Systems, Florence, Italy.

* To whom correspondence should be addressed: Institut für Biophysik und Physikalische Biochemie, Universität Regensburg, Universitätsstr. 31, D-93040 Regensburg, Germany. E-mail: hans-robert.kalbitzer@biologie.uni-regensburg.de. Phone: 0049 941 943 2594. Fax: 0049 941 943 2479.

§ University of Frankfurt.

|| University of Darmstadt.

⊥ University of Regensburg.

@ Max-Planck-Institute for Molecular Physiology.

[1] Abbreviations: *a*, (super)hyperfine coupling constant; CW, continuous wave; *D*, axial ZFS term; DSS, 2,2-dimethyl-2-silapentane-5-sulfonate; DTE, dithioerythritol; *E*, rhombic ZFS term; EPR, electron paramagnetic resonance; *g*, electron *g*-factor; GAP, GTPase-activating protein; GDP, guanosine 5′-diphosphate; GEF, guanine nucleotide exchange factor; GppNHp, guanosine 5′-O-(β,γ-imidotriphosphate); GTP, guanosine 5′-triphosphate; HPLC, high-performance liquid chromatography; Hepes, 4-(2-hydroxyethyl)-1-piperazineethanesulfonic acid; m_I, nuclear spin quantum number; m_S, electron spin quantum number; NMR, nuclear magnetic resonance; Ras, product of the ras (rat sarcoma) gene; RhoA, product of the rhoA gene; SHF, superhyperfine coupling; Tris, tris(hydroxymethyl)amimnomethane; ZFS, zero-field splitting.

10.1021/bi002164y CCC: $20.00
Published on Web 01/27/2001

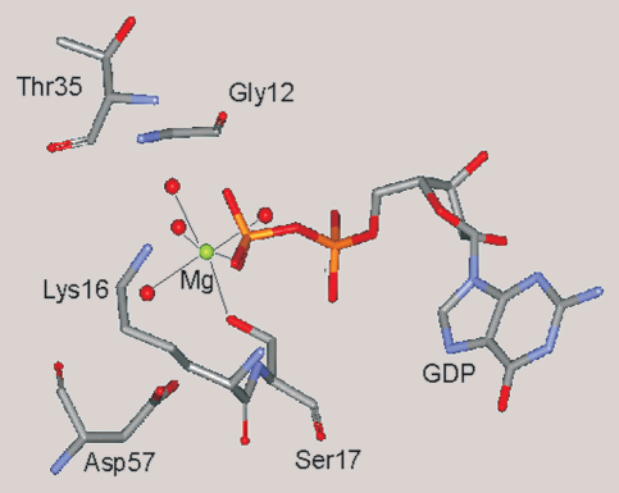

FIGURE 1: Coordination scheme of the metal−nucleotide complex from X-ray data of the Ras·Mg^{2+}·GDP complex. The data were taken from ref *4* as deposited in the Brookhaven Protein Data Bank (1q21). The water molecules coordinated to the metal ion in the X-ray structure are shown.

importance. Figure 1 shows part of the active center, as derived from the crystallographic data from Ras·GDP (*4*). In this structure, the divalent ion is coordinated to the β-phosphate group of GDP, to the hydroxyl group of Ser17, and to four water molecules. Three of the water molecules are arranged in an equatorial position, and one is positioned axially within the octahedral configuration around the central metal ion.

As formerly applied to the active form (*6*), magnetic resonance spectroscopy of the bound ligands in the Ras·Mg^{2+}·GDP complex in solution may reveal important differences beween the solution and the solid state of the Ras protein. ^{31}P NMR, for instance, is a well-suited method for observation of the phosphate groups of GDP. In contrast, the divalent ion bound to the nucleotide can preferably be observed by EPR spectroscopy after substitution of the diamagnetic magnesium ion with a paramagnetic manganese ion. Further information can be obtained by EPR after specific isotope substitution, or by exchange of normal water with ^{17}O-enriched water. The latter makes the observation of superhyperfine interactions between the metal ion and the surrounding water molecules feasible.

In the past, manganese EPR has been applied to Ras by several groups in the liquid (*7*−*9*) as well as in the frozen state (*10*−*13*). At the field strength used in the earlier studies in liquid solution, the manganese lines are too broad to extract the number of surrounding water molecules from ^{17}O superhyperfine coupling with high confidence. Since the manganese line width in solution decreases in the Ras−nucleotide complexes at high magnetic field (*6*), we applied high-field, high-frequency EPR spectroscopy at 94 GHz to study the Ras·Mn^{2+}·GDP complex at room temperature.

MATERIALS AND METHODS

Protein Purification. Wild-type and mutants of Ras (residues 1−189) were expressed in *Escherichia coli* and purified as described previously (*14*). The final purity of the protein was >95% as judged from the sodium dodecyl sulfate−polyacrylamide gel electrophoresis. The concentration of the protein solution was determined by the Bradford assay with bovine serum albumin as the standard (*15*). The amount and kind of protein-bound nucleotide were analyzed by C18 reverse-phase HPLC and quantitated with a calibrated detector (Beckman) and integrator (Shimazu).

Preparation of EPR Samples. The Ras·Mn^{2+}·GDP complex was generated by incubation of the Ras·Mg^{2+}·GDP complex in 50 mM Tris (pH 7.4), 200 mM ammonium sulfate, and a 100-fold excess of $MnCl_2$ over the protein concentration. After incubation overnight at 278 K, free metal ions were separated by gel filtration (Sephadex G-75 10/30, Pharmacia). All the buffers that were used were equilibrated with a chelating resin (Chelex 100, Bio-Rad) to remove divalent metal ions. The spectra of the proteins were recorded in 40 mM Hepes (pH 7.4) with 2 mM DTE to prevent oxidation of the protein.

Samples with $H_2{}^{17}O$ were generated by lyophilizing frozen samples and disssolving the protein in the same amount of $H_2{}^{17}O$ (46.3%). Control measurements were taken with samples of equally treated lyophilized protein which was resolved in metal ion free doubly distilled water.

Preparation of NMR Samples. To the Ras proteins in 40 mM Hepes (pH 7.4), 10 mM $MgCl_2$, and 2 mM DTE with a protein concentration of ~1 mM was added 10% D_2O to obtain a lock signal. DSS (0.1 mM) was added to calibrate the spectra by indirect referencing.

EPR Spectroscopy. CW EPR experiments were performed on a Bruker E580 spectrometer operating at 95 GHz. About 20 μL of the sample was filled in a quartz capillary with an inner diameter of 0.5 mm. All measurements were performed at 297 K, except where otherwise noted.

NMR Spectroscopy. ^{31}P NMR spectra were recorded with a Bruker DRX-500 NMR spectrometer operating at 202 MHz. Measurements were taken in a 10 mm probe using 8 mm Shigemi sample tubes filled with 1.2 mL of sample. The chemical shifts were referenced indirectly to internal DSS with a Ξ value of 0.404 807 356 1 reported by Maurer and Kalbitzer (*16*) for 85% external phosphoric acid contained in a spherical bulb. The sample temperature was varied in the range of 278−298 K.

Analysis of the EPR Data. General anlaysis of EPR spectra from high-spin ($S = {}^5/_2$, $I = {}^5/_2$) Mn^{2+} complexes have already been published in various articles [see, for instance, Reed and Markham (*17*)]. Since in this work our numerical analysis is related to experimental data taken at high magnetic fields, a pertubation theoretical treatment to the second order of the Mn hyperfine and ZFS is fully sufficient to describe the Mn^{2+} EPR spectra of the systems being investigated. The ^{17}O nuclear spin quantum number is also $^5/_2$ as for ^{55}Mn. Anisotropic contributions of g and of the Mn hyperfine coupling can be safely neglected. Furthermore, the small anisotropic contributions of the ^{17}O SHF were not explicitely taken into account in the data analysis (*18*, *19*). Because of zero-field broadening, out of 30 allowed EPR transitions only the six Mn hyperfine transitions with an $m_S = -{}^1/_2 \leftrightarrow {}^1/_2$ can be resolved in the CW EPR powder spectra.

Numerical data analysis was performed by a computer program written in MATLAB. The program is based on perturbation theory as described by Reed and Markham (*17*). It allows fitting of the experimental spectra by means of a Simplex algorithm and manual simulations by variation of the independent parameters. They are given by the isotropic ^{17}O SHF coupling, the ZFS parameters D and E, a homo-

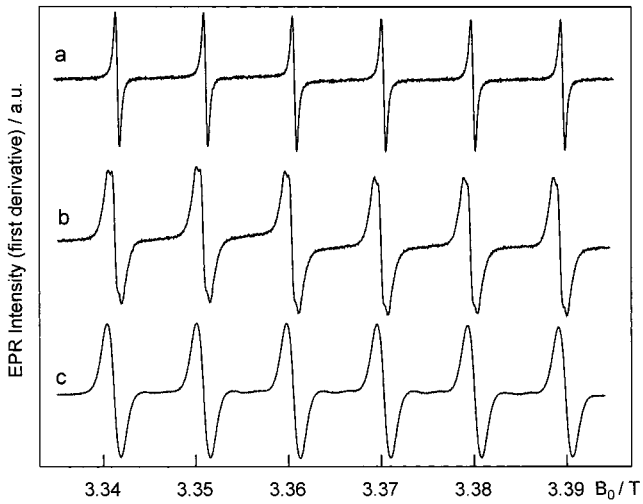

FIGURE 2: W-Band spectra of the Mn^{2+}·GDP complex of Ras in solution. (a) W-Band EPR spectrum of a solution containing 1 mM Ras(wt)·Mn^{2+}·GDP, 40 mM Hepes (pH 7.4), and 2 mM DTE. The spectra were recorded at 293 K in the liquid state. (b) Same experimental conditions and sample composition as for spectrum a but the normal water was replaced with 46.3% $H_2{}^{17}O$ enriched water. (c) Same sample as for spectrum b but measured in the frozen state at 20 K.

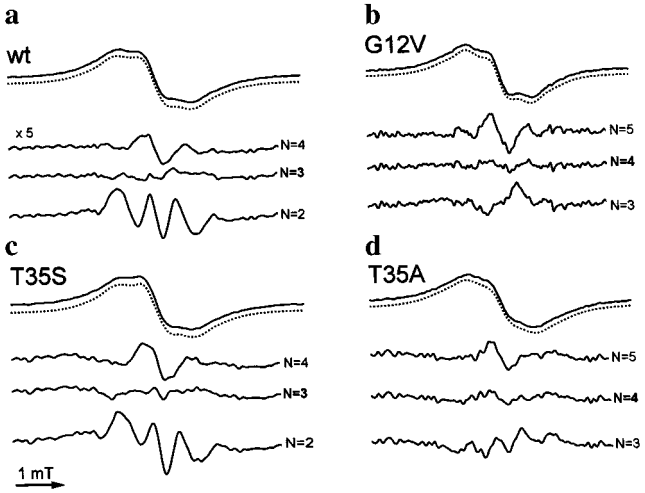

FIGURE 3: Fit of the EPR lines assuming different numbers of water ligands in the manganese hydration sphere. Sample composition and experimental conditions as described in the legend of Figure 2. Only the fourth hyperfine line is shown, on top of the experimental data (solid lines) with the best fits (dotted lines). In addition, the residuals assuming different numbers N of water ligands of the metal ion are shown. The zero-field parameter E was in all simulations close to zero; in the limits of error, $E = 0$ mT can be assumed. (a) For the Ras(wt)·Mn^{2+}·GDP complex, the best fit is obtained when $N = 3$, the zero-field splitting parameter $D = 13.6$ mT, and the $^{17}O-^{55}Mn$ SHF coupling $a = 0.274$ mT. (b) For the Ras(G12V)·Mn^{2+}·GDP complex, the best fit is obtained when $N = 4$, $D = 12.0$ mT, and $a = 0.248$ mT. (c) For the Ras(T35S)·Mn^{2+}·GDP complex, the best fit is obtained when $N = 3$, $D = 10.9$ mT, and $a = 0.277$ mT. (d) For the Ras(T35A)·Mn^{2+}·GDP complex, the best fit is obtained when $N = 4$, $D = 14.6$ mT, and $a = 0.257$ mT.

geneous line width parameter, and the number of water molecules. The program calculates powder averages with variable angular resolution to take into account randomly oriented samples. The angular dependence of the resonant field positions is solely given in our simulations by the nonvanishing quadratic ZFS interaction of Mn^{2+} that is characterized by the ZFS terms D and E.

Since no completely ^{17}O-enriched water can be obtained commercially, the hydration shell of the protein-bound manganese contains a statistical distribution of $H_2{}^{17}O$ and $H_2{}^{16}O$ molecules. With N_{H_2O} as the total number of water molecules in the first hydration shell of the manganese ion and f defined as the percentage of the ^{17}O enrichement of the water, one obtains a binomial distribution for the probability p_i for having i enriched and $N_{H_2O} - i$ nonenriched water molecules in the hydration shell. The experimental spectra are superpositions of subspectra with different numbers i of $H_2{}^{17}O$ molecules in the hydration shell weighted by the probabilties p_i.

RESULTS

EPR Spectroscopy of Wild-Type and Mutant Ras·Mn^{2+}·GDP Complexes at High Magnetic Fields. As an example, in Figure 2, the W-band EPR spectra of the wild-type Ras·Mn^{2+}·GDP complex are shown. The spectrum on the top (Figure 2a) was recorded at 293 K in normal ($H_2{}^{16}O$) water. The six dominating hyperfine lines, corresponding to the central fine structure transition $m_S = -1/2 \leftrightarrow 1/2$, are well-resolved and have line widths (measured as the separation of the maxima and minima in the first-derivative spectrum) of 0.45 ± 0.01 mT compared with a value of 0.81 ± 0.01 mT measured at Q-band frequencies of 35 GHz (*7*). After replacement of normal water by addition of ^{17}O-enriched water (46.3% $H_2{}^{17}O$), an additional signal is superimposed to the signal of normal water which is clearly visible in the room-temperature spectrum (Figure 2b). It is caused by the ^{17}O SHF contribution of $H_2{}^{17}O$ in the first coordination sphere of the bound metal ion. In the frozen state at 20 K, this signal is not resolved but can only be detected as a line broadening in the spectrum (Figure 2c).

By numerical simulation of the manganese EPR spectra, the number N of water molecules in the first hydration sphere of the bound manganese can be extracted. The SHF coupling constants published for Mn(II)$-H_2{}^{17}O$ complexes vary in the literature between 0.2 and 0.4 mT and have to be assumed as fit parameters to be optimized for integer numbers of water molecules. Very similar values for the wild-type and mutant proteins can be expected. Figure 3a shows the simulations for two, three, and four $H_2{}^{17}O$ ligands together with the experimental data recorded from the Mn^{2+}·GDP complex with Ras(wt). In contrast to the coordination scheme derived from the X-ray structure (Figure 1), which contains four water molecules in the first coordination sphere, only the assumption of three water molecules in the relevant sphere allows a satisfying fit of the data. In contrast, two Q-band EPR studies by Smithers et al. (*8*) and Latwesen et al. (*9*) performed under similar experimental conditions describe the detection of four water molecules in the first coordination sphere of the metal ion in the Ras·Mn^{2+}·GDP complex. However, these data were derived from oncogenic variants of the protein, containing the mutations G12R/A59T, A59T, and G12V/A59T, respectively (*20*). These mutations decrease the hydrolysis rate of GTP bound at the active site and may therefore also have an influence on the coordination of the metal ion bound to the nucleotide. Two of them contain a mutation of Gly12 whose replacement with amino acids other than proline always leads to an oncogenic activation of Ras. Therefore, we investigated the single mutant Ras(G12V); in

Table 1: Number of Water Molecules Coordinated to the Metal Ion in Wild-Type and Mutant Ras·Me^{2+}·GDP Complexes and ^{31}P NMR Data of the Bound Nucleotide[a]

sample	N (H_2O)	α-phosphate group δ_1 (ppm)/δ_2 (ppm)	β-phosphate group δ_1 (ppm)	β-phosphate group δ_2 (ppm)	$K_1(1,2)$
Ras(wt)·Me^{2+}·GDP	3	−10.68	−2.00	−2.15	0.31
Ras(T35S)·Me^{2+}·GDP	3	−10.71	−2.04	−2.19	0.21
Ras(T35A)·Me^{2+}·GDP	4	−10.70	−2.06	−2.19	0.49
Ras(G12V)·Me^{2+}·GDP	4	−10.60	−1.78	−	<0.04

[a] The number of water molecules N in the first coordination sphere of the metal ion Me^{2+} is taken from the EPR experiments, where state 1 is defined as the state with the β-phosphate resonance shifted downfield relative to that of state 2. δ_1 and δ_2 are the corresponding chemical shifts. $K_1(1,2)$ is the equilibrium constant between state 1 and state 2 defined by [2]/[1]. The data were fitted with a coupling constant $^2J_{\alpha\beta}$ of 15.8 Hz. The chemical shifts were determined at 298 K and are indirectly referenced to internal DSS.

agreement with the published data, we find one additional water molecule bound to the metal ion in this mutant (Figure 3b and Table 1).

Apparently, point mutations of amino acids not coordinated directly to the metal ion can strongly influence the ligand sphere of the metal ion. To further elucidate the structure of the GDP form of the protein near the metal ion, we have investigated site-specific mutants of the protein. The mutants were studied under conditions identical to those described above for the wild-type system. The mutant T35A was chosen since alanine lacks the OH group available in threonine which is assumed to be important for triggering the conformational change induced by triphosphate binding (*21*). The second mutant T35S is very similar to the wild-type protein since it still contains the hydroxyl group in position 35 and only lacks the hydrophobic methyl group of threonine. In line with this expectation, the EPR spectra of wild-type protein and the T35 mutants, measured with ^{17}O-enriched water, confirm these differences and immediately provide direct evidence for changes in the environment of the metal ion. Whereas the data of the serine mutant can be fitted optimally assuming three water ligands (Figure 3c), that is, with the same number of water molecules as found for the wild-type protein, a satisfactory fit for the alanine mutant can only be obtained by assuming an additional water molecule in the hydration shell of manganese (Figure 3d). As expected, the magnitude of the obtained SHF coupling constant is very similar to that obtained for the wild-type protein as well as for the serine mutants. Furthermore, it should be noted that solutions assuming two or three water molecules do not lead to satisfactory simulations, independent of the assumed $^{17}O-^{55}Mn$ superhyperfine coupling constant. This can be seen in the corresponding residue shown in Figure 3, where the SHF coupling was a free fit parameter for each of the accounted integer numbers of water molecules.

^{31}P NMR Spectroscopy. Additional information about the active site can be gained from the observation of the phosphate groups by ^{31}P NMR spectroscopy (Figure 4). A pattern similar to that observed by EPR spectroscopy can be found with respect to the comparison of the Ras(wt) and mutant spectra; the spectra of Ras(wt) and Ras(T35S) are almost identical, whereas the spectra of mutants Ras(G12V) and Ras(T35A) clearly differ from the wild-type spectra. First, this observation supports the assumption that the differences as detected by high-field EPR are not related to the replacement of the naturally occurring Mg^{2+} ion with Mn^{2+}. Furthermore, a careful inspection of the resonance

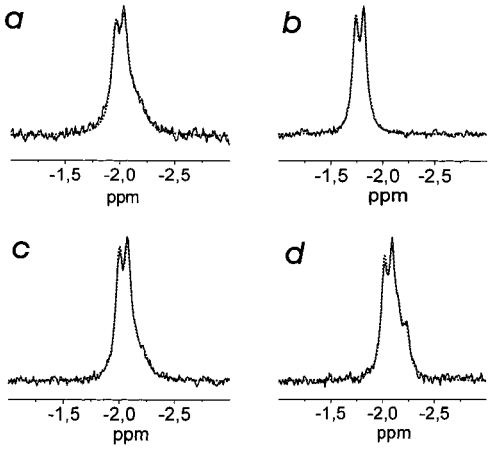

FIGURE 4: ^{31}P NMR spectra of wild-type and mutant Ras·Mg^{2+}·GDP complexes. ^{31}P NMR spectra of a solution containing 1 mM Ras, 40 mM Hepes (pH 7.4), 10 mM $MgCl_2$, and 2 mM DTE. The ^{31}P NMR spectra were recorded at 298 K in the liquid state. The experimentally obtained β-phosphate lines of the (a) Ras(wt)·Mg^{2+}·GDP, (b) Ras(G12V)·Mg^{2+}·GDP, (c) Ras(T35S)·Mg^{2+}·GDP, and (d) Ras(T35A)·Mg^{2+}·GDP complexes are shown together with the best fits to the data assuming two states (dotted lines). The signal-to-noise ratio was improved by exponential filtering, leading to an additional broadening of 2 Hz. Data were fitted with the parameters given in Table 1. The indirect spin−spin coupling constant $^2J_{\alpha\beta}$ taken from the fit of the best-resolved spectrum [Ras(G12V)] is 15.8 ± 0.1 Hz; in the limits of error, the same coupling constants were obtained for the other fits.

line of the β-phosphate group of GDP bound to Ras(T35A) reveals that this mutant occurs in two different conformational states, showing up as a partially superpositioned pair of resonance lines. Such a conformational equilibrium has been observed earlier for Ras with a nucleoside triphosphate bound (*6*). From a fit of the data, one can calculate the equilibrium constant $K_1(1,2)$ for the two states, which is 0.49 at 298 K (Table 1). If it is assumed that the line width is completely determined by exchange broadening, an upper limit for the exchange rate constant k_1 at 298 K can be estimated to be 40 s^{-1}. However, the real rate constant should be appreciately smaller, since the ^{31}P NMR line widhts of the protein-bound nucleotide should be rather large. Using the line width of Ras(G12V) as a plausible estimate for the natural line width in the absence of exchange broadening leads to a value for k_1 of approximately 3 s^{-1}. The second state seems also to exist in Ras(wt) and Ras(T35S) but with a smaller population. In the mutant Ras(G12V), there is no indication of a second conformational state, and a decrease in the relative chemical shift further points to changes in the surroundings of the β-phosphate group in this mutant.

Putting together the EPR and NMR data, we find the most remarkable results are the differences between the wild-type protein Ras(wt) and the oncogenic mutant Ras(G12V), which can clearly be detected by NMR as well as by high-field EPR at room temperature. The conformational differences between the wild-type system and these mutants have not been detected by X-ray structure analysis and may be related to important functional changes in the oncogenic mutant. The conformational changes must thereby obviously alter at least one of the direct ligands to the metal ion and furthermore influence the conformation nearby the β-phosphate of the nucleotide, which can be deduced from the prominent differences visible in the NMR spectra of Ras(G12V) and Ras(T35A).

DISCUSSION

Our data show that at room temperature the manganese ion is complexed with three water molecules in the GDP complex of wild-type H-Ras. The same coordination pattern is found for the point mutant T35S. The replacement of the threonine residue with alanine, a residue without a hydroxyl group, leads to an increase in the hydration number of one. Since the coordination number of manganese as well as magnesium is known to be six in these systems, three or two non-water ligands are to be expected. If one compares the data from solution with the data from X-ray crystallography (*4*, *5*), it is clear that in the wild-type protein one of the ligands should be an oxygen of the β-phosphate group of GDP (Figure 1). This has also been shown to be true in solution by EPR spectroscopy using regiospecifically ^{17}O-labeled [β-$^{17}O_4$]GDP in cellular wild-type H-ras as well as in the oncogenic mutants G12V, G12R/A59T (*7*), and G12V/A59T (*9*). According to all crystal structures published so far, the hydroxyl group of Ser17 is coordinated to the metal ion. In two of the published X-ray structures, the remaining coordination sites are occupied by water molecules; only the structure by Schlichting et al. (*5*) exhibits a second coordination from the protein to be the side chain carboxyl group of Asp57. Our data would indicate the latter cordination scheme may be preserved in solution.

At first glance, our EPR results seem to disagree with the published results of EPR experiments which found four water molecules in the first hydration sphere. However, we could show that mutations of amino acids near the nucleotide binding site, such as mutations of Gly12 or Thr35, can increase the number of water molecules. Since the Q-band EPR studies in liquid solution published by Reed's group (*8*, *9*) were also performed on oncogenic mutants, changes in the coordination sphere of the metal ion as caused by these mutations can now be predicted from the room-temperature EPR investigations. On the other hand, a high-field EPR study on frozen solutions of N-Ras resulted in a best fit of the data when assuming four water molecules in the first hydration shell of manganese (*11*). As we pointed out above, the spectral resolution in frozen solutions decreases considerably as compared to that of room-temperature spectra, and thus, the significance of the data analysis decreases as well. Accordingly, we cannot distinguish from simulations of our high-field EPR spectra taken on frozen solutions (simulations not shown) whether three or four water molecules are coordinated. Inhomogeneous contributions from anisotropic SHF couplings, higher-order ZFS, and ZFS strains might broaden and complicate the frozen solution spectra. Alternatively, or in addition, the coordination structure of the metal ion may be altered upon freezing the protein. The latter explanation seems likely since it could also be the reason for the different conformations detected by X-ray structure analysis, which are commonly taken at very low temperatures.

In one of the published X-ray structures (*6*), on the other hand, differences between the wild-type protein and the oncogenic mutant G12V are reported in a region around Asp57. According to this study, Asp57 is directly coordinated to the metal ion in the GDP form but via an intervening water molecule in the GTP form. Three water ligands are also found in the X-ray structures from the Mg^{2+}·GDP complex of the human small GTPase RhoA (*22*), where the main chain carboxyl of Thr35 is directly coordinated to the metal ion.

In line with the hypothesis that Ras may be able to exist in more than one conformational state in solution, our NMR experiments unambiguously show that Ras(T35A) occurs in two different conformations which are interconverting rather slowly ($k_{1-1} \sim 3\ s^{-1}$). This is most probably also true for the wild-type protein, although the population of the second state is much smaller (Table 1). If the Ras·Mg^{2+}·GDP complex exists in more than one conformation, one may ask what the biological sense of such a conformational heterogeneity can be. When the Ras activation−deactivation cycle is considered, it is evident that at least two different states have to exist which are different from the main equilibrium state: (1) the state directly after the GTP hydrolysis and before the release of the phosphate group and (2) the open state of the molecule just before the release of GDP which is then physiologically replaced with GTP. Further investigations are necessary to correlate these functional states with our results; a detailed study of the kinetics of mutants such as Ras(T35A) may provide a clue about the answer to these questions.

ACKNOWLEDGMENT

We gratefully acknowledge Norbert Weiden and Klaus Peter Dinse (TU-Darmstadt) for their contributions to recording of the W-band spectra in their laboratory. This work was supported by the Deutsche Forschungsgemeinschaft (Schwerpunktprogramm "Hochfeld EPR in Biologie, Chemie und Physik").

REFERENCES

1. Boguski, M. S., and McCormick, F. (1993) *Nature 366*, 643−654.
2. Wittinghofer, A., Scheffzek, K., and Ahmadian, M. R. (1997) *FEBS Lett. 408*, 315−318.
3. Milburn, M. V., Tong, L., de Vos, A. M., Brünger, A., Yamaizumi, Z., Nishimura, S., and Kim, S.-H. (1990) *Science 247*, 939−945.
4. Tong, L., deVos, A. M., Milburn, M. V., Brunger, A., and Kim, S.-H. (1991) *J. Mol. Biol. 271*, 503−516.
5. Schlichting, I., Almo, S. C., Rapp, G., Wilson, K., Petratos, K., Lentfer, A., Wittinghofer, A., Kabsch, W., Pai, E. F., Petsko, G., and Goody, R. S. (1990) *Nature 345*, 309−315.
6. Geyer, M., Schweins, T., Herrmann, C., Prisner, T., Wittinghofer, A., and Kalbitzer, H. R. (1996) *Biochemistry 35*, 10308−10302.
7. Feuerstein, J., Kalbitzer, H. R., John, J., Goody, R. S., and Wittinghofer, A. (1987) *Eur. J. Biochem. 162*, 49−55.

8. Smithers, G. W., Poe, M., Latwesen, D. G., and Reed, G. H. (1990) *Arch. Biochem. Biophys. 280*, 416−420.
9. Latwesen, D. G., Poe, M., Leigh, J. S., and Reed, G. H. (1992) *Biochemistry 31*, 4946−4950.
10. Larsen, R. G., Halkides, C. J., and Singel, D. J. (1993) *J. Chem. Phys. 98*, 6704−6721.
11. Bellew, B. F., Halkides, C. J., Gerfen, G. J., Griffin, R. G., and Singel, D. J. (1996) *Biochemistry 35*, 12186−12193.
12. Halkides, C. J., Bellew, B. F., Gerfen, G. J., Farrar, C. T., Carter, P. H., Ruo, B., Evans, D. A., Griffin, R. G., and Singel, D. J. (1996) *Biochemistry 35*, 12194−12200.
13. Farrar, C. T., Halkides, C. J., and Singel, D. J. (1997) *Structure 5*, 1055−1066.
14. Tucker, J., Sczakiel, G., Feuerstein, J., John, J., Goody, R. S., and Wittinghofer, A. (1986) *EMBO J.*, *5*, 1351−1358.
15. Bradford, M. M. (1976) *Anal. Biochem. 72*, 248−254.
16. Maurer, T., and Kalbitzer, H. R. (1996) *J. Magn. Reson., Ser. B 113*, 177−178.
17. Reed, G. H., and Markham, G. D. (1984) *Biol. Magn. Reson. 6*, 73−142.
18. Tan, X., Poyner, R., Reed, G. H., and Scholes, C. P. (1993) *Biochemistry 32*, 7799−810.
19. Tan, X., Bernardo, M., Thomann, H., and Scholes, C. P. (1995) *J. Chem. Phys. 102*, 2675−2690.
20. John, J., Frech, M., and Wittinghofer, A. (1988) *J. Biol. Chem. 263* (24), 11792−11799.
21. Wittinghofer, A., and Pai, F. (1991) *Trends Biochgem. Sci. 16*, 382−387.
22. Wei, Y., Zhang, Y., Derewenda, U., Liu, X., Minor, W., Nakamoto, R. K., Somlyo, A. V., Somlyo, A. P., and Derewenda, Z. S. (1997) *Nat. Struct. Biol. 4*, 699−703.

BI002164Y